Polymer 50 (2009) 1957–1964

Contents lists available at ScienceDirect

Polymer

journal homepage: www.elsevier.com/locate/polymer

Change of structure and free volume properties of semi-crystalline poly(3-hydroxybutyrate-co-3-hydroxyvalerate) during thermal treatments by positron annihilation lifetime

Mei-Ling Cheng [a], Yi-Ming Sun [a,b,*], Hongmin Chen [c], Y.C. Jean [b,c]

[a] Department of Chemical Engineering and Materials Science, Yuan Ze University, Chung-Li, Taoyuan 32003, Taiwan
[b] R&D Center for Membrane Technology, Chung Yuan University, Chung-Li, Taoyuan 32023, Taiwan
[c] Department of Chemistry, University of Missouri-Kansas City, Kansas City, MO 64110, USA

ARTICLE INFO

Article history:
Received 10 September 2008
Received in revised form
12 February 2009
Accepted 14 February 2009
Available online 26 February 2009

Keywords:
Positron annihilation lifetime
Free volume
Rigid amorphous fraction

ABSTRACT

The structure and free volume properties of semi-crystalline poly(3-hydroxybutyrate-co-3-hydroxyvalerate) (PHBV) were investigated in this study. The structure change and conformational motion of PHBV during melting and crystallization process were discussed by in situ FTIR. The free volume within the amorphous phase and its temperature dependence in the PHBV membrane, which was prepared by the compression molding method with isothermal crystallization processes, were characterized by using positron annihilation lifetime (PAL) spectroscopy. From the lifetime parameters, the temperature dependence of free volume size, amount, distribution, and fractional free volume, and the thermal expansion of free volume and/or polymer were discussed. Furthermore, the knee temperature was first observed in the melting process of the crystallized PHBV membranes. It indicated that there was structural transition of polymer chains during melting as the corresponding results observed with in situ FTIR measurement.

1. Introduction

Polyhydroxyalkanoates (PHAs) are a class of biological polyesters. They represent a diverse group of energy storage compounds in bacteria, and they are commonly accumulated when carbon and energy sources are available in excess but the supply of an essential nutrient, such as nitrogen, phosphorus, and sulfur is limited. Because they are produced from renewable carbon sources and can be biodegraded to carbon dioxide and water, PHAs are often considered as eco-friendly polymers, and expected to contribute to the construction of environmentally-sustainable society. In addition to the remarkable characteristics of the biodegradability and recyclablility of PHAs, the rate of biodegradation of PHAs in moist air is negligible and their shelf life is adequate for most end uses. These features make PHAs especially suitable for use as packaging materials.

Among the family of PHAs, poly(3-hydroxybutyrate) (PHB) and poly(3-hydroxybutyrate-co-3-hydroxyvalerate) (PHBV) copolymers have received earliest attention since their discovery. PHB is highly crystalline (near 80%) with a melting temperature close to 180 °C, so that it is hard and brittle [1]. However, the introduction of different HA monomers such as 3-hydroxyvalerate (3HV) or 3-hydroxyhexanoate (3HHx) into the chain greatly improves the material properties of PHB. PHBV copolymers were once commercially known as Biopol®, and they could offer a range of physical properties from relatively brittle PHB and low 3HV content copolymers to the more flexible and tougher high 3HV grades [2]. A number of reports have shown that PHBV copolymers offer interesting barrier properties for water and gases [3,4]. The gas barrier property is useful for application in food packaging and for making plastic beverage bottles. It has also been exploited to make coated paper and films which are used for coated paper milk cartons [5].

The distribution and size of free volume holes are the most important characteristic to describe the transport of small molecules, such as gases and a number of solvents, in a nonporous polymer matrix. For studying the free volume properties of polymers, the positron annihilation lifetime (PAL) spectroscopy method has been developed to be an important tool during the past two decades [6–10]. In molecular solids and liquids, a fraction of the

* Corresponding author. Department of Chemical Engineering and Materials Science, Yuan Ze University, 135 Yang Tun Road, Chung-Li, Taoyuan 32003, Taiwan. Tel.: +886 3 4638800x2558; fax: +886 3 4559373.
E-mail address: cesunym@saturn.yzu.edu.tw (Y.-M. Sun).

0032-3861/$ – see front matter © 2009 Elsevier Ltd. All rights reserved.
doi:10.1016/j.polymer.2009.02.025

positrons injected from a radioactive source forms a bound state with an electron before annihilation, which yields a positronium, Ps. Positroniums may be formed into different states: *para*-positronium (*p*-Ps, singlet state) for antiparallel spins and *ortho*-positronium (*o*-Ps, triplet state) for parallel spins. Three components appear in the lifetime spectra of amorphous polymers, and these are attributed to the annihilation of *p*-Ps, free positrons, and *o*-Ps. *p*-Ps decays mainly via self-annihilation with a lifetime of about 0.125 ns. Free positrons annihilate with lifetime in the rage of 0.3–0.4 ns. The intrinsic vacuum lifetime of *o*-Ps is 142 ns, however, it decreases typically to a few nanosecond range in matters. This is due to collisions of Ps with molecules (pick-off annihilation) [11]. If *o*-Ps localized at a free volume hole in the amorphous polymer, its lifetime is between 2 and 5 ns, and highly sensitive to the size of these free volume.

In semi-crystalline polymers, according to the unique crystalline structure, which are lamellae and/or spherulites, the amorphous phase existed between crystalline regions. The non-crystalline phase must be subdivided into the non-crystalline amorphous and the crystalline-amorphous interfacial portions. The cause for the interfacial region is the continuation across the phase boundaries of the molecules which are much longer than the phase dimensions. This region is amorphous but has a constrained molecular mobility, due to the presence of crystallinity, and is usually described as rigid-amorphous fraction (RAF) [12]. In addition, the non-crystalline amorphous region is liquid-like amorphous and expected to behave properties normally, such as T_g, as the completely amorphous bulk polymers. It may be termed as mobile amorphous fraction (MAF). The concept of RAF in addition to crystalline phase and MAF has been investigated to explain properties of semi-crystalline polymers in recent years [7,13–15]. Accordingly, the situation of free volume of semi-crystalline polymers appears to be much more complex due to the presence of crystallites and amorphous regions of different mobilities.

Because of the structure of semi-crystalline polymer, positroniums may be formed in both the crystalline and amorphous phases. The possible regions with free volume holes probed by *o*-Ps are (1) open amorphous texture and interfaces in spherulites, (2) interlamellar phase and lamellar defects, and (3) interstitial cavity in the crystalline unit cell [16]. For *p*-Ps and free positron annihilation, the lifetimes may be much close as annihilating in those regions due to the self-annihilation of *p*-Ps and free positron. But, the lifetimes of *o*-Ps in crystalline and amorphous phases may be different because of the high response of the pick-off annihilation rate to different packing densities [17]. In this way, the microstructure of the crystalline and amorphous phases which contain the MAF and RAF can be studied.

In this work, the formulation of the structural three-phase model for semi-crystalline PHBV, including MAF, RAF, and crystalline region, is addressed to interpret the free volume characteristics of the melt-crystallized PHBV membranes. It is achieved via a systematic study of the temperature dependence of free volume holes between 25 and 190 °C. The aim of this study is to probe the structural change of the polymer at the nanoscale and/or molecular levels during crystallization and melting processes of PHBV polymer. Also, the potential and limit of PAL for studying the thermal expansion and melting behavior in semi-crystalline polymers are investigated. Moreover, a "knee" temperature, T_k, where the increase of *o*-Ps lifetime with temperature levels off is paid attention. This critical temperature has already been mentioned in some semi-crystalline polymers previously, such as poly(ε-caprolactone) [18], polypropylene [19], etc. Thus, a second aim of this work is tried to figure out the leveling-off effect of *o*-Ps lifetime in PHBV polymer. Herein, the conformational change of molecular chain observed by in situ FTIR is discussed to interpret the leveling-off effect of *o*-Ps lifetime from PAL analysis.

2. Experimental

2.1. Characterization of poly(3-hydroxybutyrate-co-3-hydroxyvalerate)

Poly(3-hydroxybutyrate-co-3-hydroxyvalerate) (PHBV) was purchased from Aldrich, Inc. (USA). The 3-hydroxyvalerate (3HV) content of PHBV was 5 mol% determined by ^{1}H NMR spectra. The weight-average molecular weight ($\overline{M}_w$) was about 400,000 g/mol and the polydispersity index (*PDI*) was about 2 as determined by gel-permeation chromatography (GPC). The temperature dependence of the PHBV polymer chain conformation was studied via FTIR-microscope (Perkin–Elmer, USA) equipped with a liquid nitrogen cooled mercury cadmium telluride (MCT) detector and a hot stage (N187 0184, Perkin–Elmer, USA). The hot stage consists of a temperature controller and a heating block that accepts infrared windows. PHBV sample was crystallized well and annealed at ambient temperature for such a long time before FTIR analysis. According to the WAXD pattern of PHBV sample (data not shown here), a fine crystal structure was observed. Disc of PHBV/potassium bromide (KBr) (1/100 by wt.) tablet sample was made and then sandwiched between two calcium fluoride (CaF_2) windows. The sample was treated with a thermal cycle, first heated stepwise from 25 to 200 °C with a heating rate of about 10 °C/min and recorded at 25, 50, 100, 125, 150, 160, 170, 180, 190, and 200 °C, respectively. The FTIR spectra were collected by the transmission mode and a signal averaging 64 scans at a resolution of 4 cm^{-1} in the wave number range of 4000–700 cm^{-1}. After melting at 200 °C for 5 min, the sample was cooled down to 40 °C with a cooling rate about 10 °C/min and recorded at 190, 180, 170, 160, 150, 125, 100, 80, 60, 40, and 28 °C, respectively. Then the sample was kept at 28 °C for 5 min. Subsequently, a second heating treatment and reverse cooling run were carried out. Data were processed with the Spectrum One software supplied by Perkin–Elmer.

Thermal characterization was carried out with a DSC instrument (Perkin–Elmer DSC7, equipped with an intra-cooler). The equipment was calibrated with indium standard. The membranes of approximately 6.0 mg were hermetically sealed in an aluminum pan for the measurements. Under a nitrogen atmosphere, samples were scanned from −40 °C to 200 °C with a rate of 10 °C/min, kept at 200 °C for 5 min, and then cooled to −40 °C with a cooling rate of 10 °C/min. Followed the cooling step, sample was placed at −40 °C for 5 min and then heated again from −40 to 200 °C with a scanning rate of 10 °C/min. The melting temperature (T_m) and the apparent enthalpy of fusion (ΔH_f) were determined from the endothermic peak on the DSC curves.

2.2. Membrane preparation

PHBV membranes were prepared by a compression-molding method performed with a molding test press (GT-7014, Gotech, Taiwan). The polymer powder was sandwiched between two flat stainless steel plates and then the plate molding assembly was placed in the hot press. The samples were melted at 170 °C for 5 min (above the melting point of PHBV, T_m, measured at 162 °C), and then were compression-molded under a pressure of 9.8 MPa at 170 °C for 15 min. Once melted, the molding assembly was removed from the hot press machine and put into an oven at 90 °C. The membrane was placed in the oven for 48 h to complete the isothermal crystallization treatment. After crystallization process, the membrane was kept in a desiccator before further characterization. The thickness of the membranes averaged around 55 μm.

2.3. Positron annihilation lifetime spectroscopy

Positron annihilation lifetime (PAL) measurements were taken by a fast–fast coincident timing spectrometer assembled with Ortec

parts (Ametek, Oak Ridge, USA). The PAL spectrometer was calibrated using a time calibrator to obtain the ratio between time and channel. All lifetime spectra were binned into 1024 channels, with a channel width of 51 ps. The resolution of the PAL was determined by measuring ^{60}Co (Isotope Products Laboratory, Burbank, USA). It was found that the full width at half maximum (FWHM) of the spectrum was 300 ps.

The positron source, ^{22}Na, is commercially available as aqueous solution of ^{22}NaCl (Isotope Products Laboratory, Burbank, USA). Approximately 20 μCi ^{22}Na was dropped onto a Kapton® (DuPont, Texas, USA) foil of 6 μm thickness. After water evaporated, the Kapton® foil was covered by another foil and the source was wrapped inside the foil and sealed. PHBV membrane samples (1.5×1.5 cm^2) were stacked to exceed 500 μm and the ^{22}Na positron source was sandwiched between the two identical polymer membrane stacks. For temperature control, the sandwiched sample was enclosed into an aluminum heating block with a PID temperature controller (BTC-9100, Brainchild Electronic Co., LTD., Taiwan). Temperature dependence of PALS measurements was carried out from 25, 35, 50 °C to 190 °C with an increment 20 °C. The PAL spectrum measurement was performed after the temperature had been stabilized. Two million counts of positron annihilation were collected in about 2 h for each spectrum.

3. Results and discussion

Fourier transform infrared (FTIR) spectroscopy is sensitive to local molecular environment and has been widely applied to examine the conformational change of macromolecules during thermal process [20,21]. In addition, FTIR has been applied to the quantitative study of polymer crystallization [21,22]. In this study, the structural change of PHBV during melting and crystallization process was discussed by in situ FTIR. Fig. 1 shows the temperature-resolved stretching vibration of the carbonyl group in PHBV during the heating process. The absorbance bands at 1724 and 1741 cm^{-1} are assigned to the vibration of C=O in the crystalline and amorphous phases, respectively. In the crystalline phase, segments formed orthorhombic unit cells, and each of which contained two left-handed helices. The oxygen atoms of C=O are located closer to the hydrogen atoms at the other segments during which the dipole moment decreased, thus resulted in a lower wave number [23]. During melting, the helical structure of PHBV disappeared gradually, leading to the band of C=O shift from 1724 to 1741 cm^{-1}.

Fig. 2 shows the fingerprint region of PHBV in the FTIR spectra. The band at 1280 cm^{-1} is assigned to the CH_2 wagging which is intensified for the CH_2–CO group and split into two bands at 1258 and 1302 cm^{-1} after melting [24]. The band at 1230 cm^{-1} is proposed as the conformational CH_2 group of the helical chains and therefore is absent in the amorphous region [24,25]. The bands at 1182 and 1131 cm^{-1} are the characteristic of the asymmetric and the symmetric stretching vibration of the C–O–C group, respectively [26]. Accordingly, the absorbance of the crystalline bands was calculated to study the melting and crystallization of PHBV as shown in Fig. 3. At first heating (Fig. 3(a)), the absorbance of all crystalline bands kept constant below 130 °C and it decreased gradually above 130 °C until melting completely. The band at 1453 cm^{-1}, which is assigned to the scissoring vibration of CH_2 group, was taken as the reference peak because it's unconcerned with the conformation of PHBV. The results presented that the helical structure broke up partially above 130 °C, and then melted completely near 170–180 °C. Afterward, the molten sample was cooled to ambient temperature and the crystallization process was shown in Fig. 3(b). During the crystallization, the amorphous C=O band gradually shifted to lower wavenumbers and presented an abrupt decrease of absorbance of 1741 cm^{-1} below 130 °C. The band shift in this region is due to the phase transition from an amorphous to a crystalline state. Other amorphous bands (1258 and 1302 cm^{-1}) didn't show significant change until cooling to 40 °C. The crystalline bands at 1230 and 1280 cm^{-1} didn't appear either. These results indicated that the C=O stretching vibration band was the most sensitive to represent the degree of the crystallization among all the bands.

Fig. 3(c) shows the absorbance change of crystalline bands during the 2nd heating process. The absorbance of the peak at 1230 cm^{-1} increased slightly while heated up to 80 °C due to further crystallization. The absorbance of the peak at 1724 cm^{-1} increased slightly while heated up to 100 °C due to further crystallization. It is noticed that the values of absorbance of crystalline bands in the second heating process were lower than that in the first heating process. That also illustrates the degree of crystallization of PHBV during the second heating process was lower than that during the first heating process. On the other hand, a distinct drop of all crystalline band absorbance was determined at 170 and 160 °C for the first and second heating, respectively (Fig. 3(a) and (c)). It is in agreement with the DSC results of PHBV sample as shown in Fig. 4. The melting temperature (T_m) of PHBV during the first heating is 161 °C and two T_ms (150 and 165 °C) are present during the second heating process. Because of less crystallization time for the PHBV sample, the crystallized sample with less perfect crystals will melt at lower temperature during the 2nd heating than the T_m of the 1st heating process.

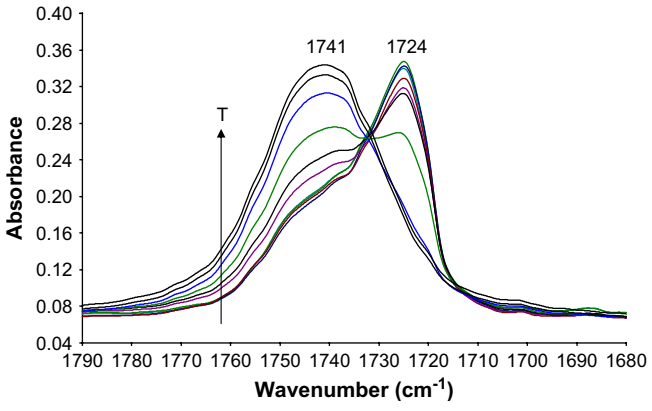

Fig. 1. The C=O band in FTIR spectra of PHBV polymer at various temperatures (25, 50, 100, 125, 150, 160, 170, 180, 190, and 200 °C from bottom to top, respectively).

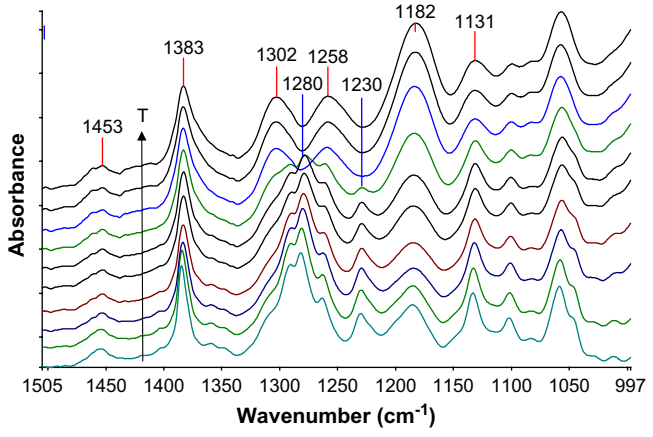

Fig. 2. FTIR spectra of PHBV polymer at various temperatures (25, 50, 100, 125, 150, 160, 170, 180, 190, and 200 °C from bottom to top, respectively).

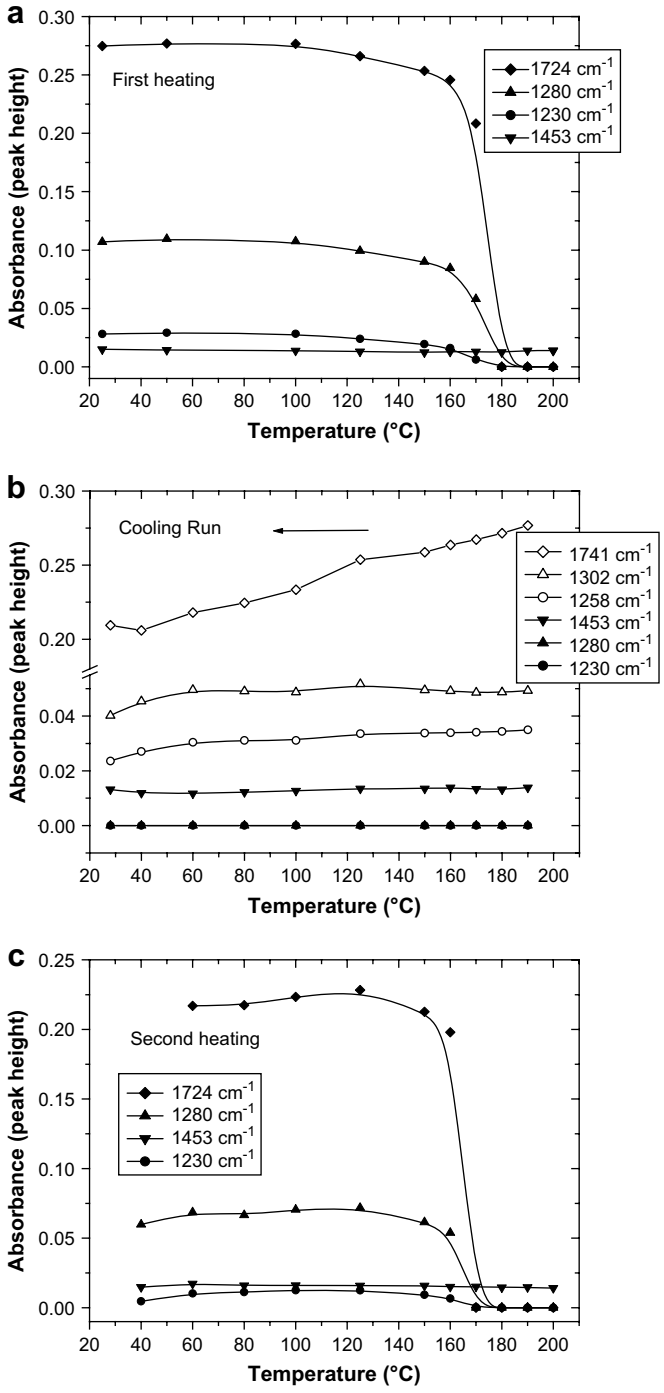

Fig. 3. Temperature dependence of crystalline sensitive bands in FTIR spectra: (a) first heating, (b) cooling run, and (c) second heating.

Moreover, the relative crystallinity of PHBV polymer could be calculated from the intensities of the amorphous and the crystalline bands. There were significant changes with temperature between the relative intensities of the bands at 1182 and 1131 cm^{-1} which are crystalline sensitive C–O–C bands. Herein, the corrected absorbance of peaks at 1131 and 1182 cm^{-1} was calculated by the baseline range from 1158 to 1113 cm^{-1} and from 1214 to 1158 cm^{-1}, respectively. With increasing temperature, the baseline of peak at 1182 cm^{-1} changed slightly (1228–1153 cm^{-1}). The variation between those values calculated under different baselines is within only 4% of peak height and can be considered negligible. The ratio of

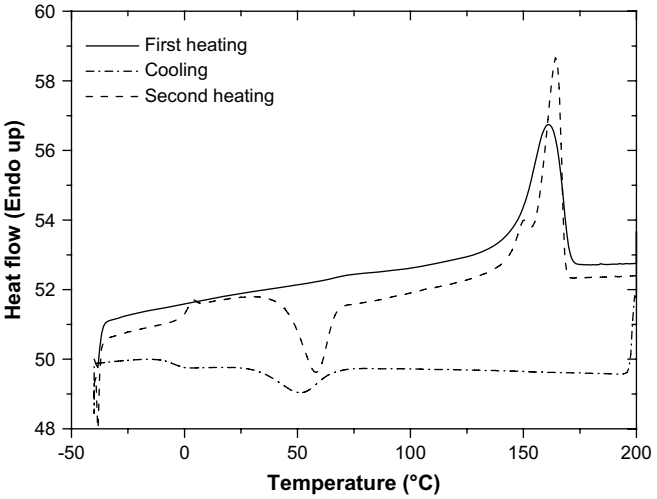

Fig. 4. Typical DSC curves of PHBV polymer (scanning rate: 10 °C/min): solid-first heating; dash dot-cooling; dash-second heating.

A_{1131}/A_{1182} versus temperature is shown in Fig. 5. It illustrates the relative measure of the degree of crystallinity and melting behavior during the thermal process clearly. From the first heating process, the relative crystallinity increased until 100 °C. The conformational change of C–O–C group shows the further crystallization obviously. As mentioned above, the crystallinity of PHBV during the first heating process was higher than that during the second heating process. Consequently, the results from FTIR provided useful information about crystallization and melting behavior of PHBV.

A series of positron annihilation lifetime (PAL) spectra for PHBV membranes, made by the isothermal crystallization process at 90 °C, at various measuring temperatures were collected and shown in Fig. 6. In some semi-crystalline polymers an intermediate (~1 ns) *o*-Ps lifetime appears, which is contributed to *o*-Ps formed in crystals, such as poly(tetrafluoroethylene) (PTFE) [7,27] and polyethylene (PE) [17,28]. However, only one *o*-Ps lifetime was observed for poly(aryl ether ether ketone) (PEEK). The intensity of *o*-Ps annihilation, which was attributed to the amorphous phase only, decreased linearly with increasing crystallinity. It has been concluded that *o*-Ps is not formed in PEEK crystal due to the dense

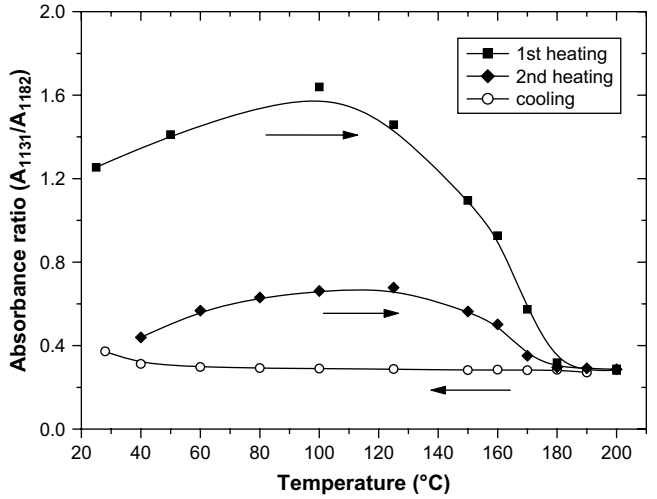

Fig. 5. Temperature dependence of absorbance ratio of A_{1131}/A_{1182} in FTIR spectra during the heating process.

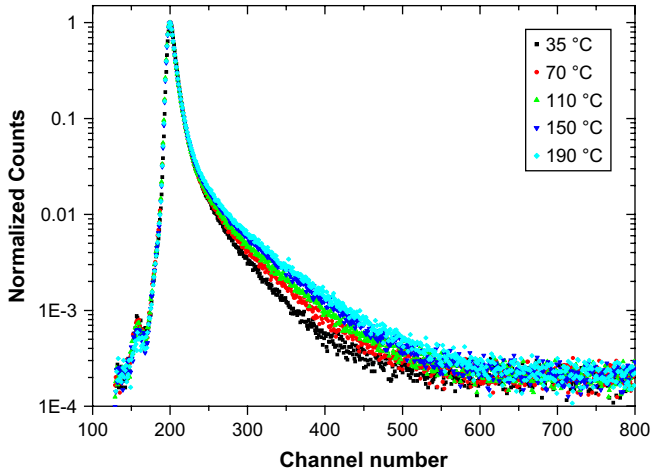

Fig. 6. Raw PAL spectra of the 90 °C isothermally crystallized PHBV membrane at various measuring temperatures.

packing [29]. This conclusion is also in agreement with investigations of semi-crystalline polyamide [30], poly(ε-caprolactone) [18] and some other semi-crystalline polymers. It is noticed that PE and its copolymers also have been analyzed into three lifetimes [14,31]. The different structure of PE (linear or branch) and dense packing may be the possible reasons for the different results of *o*-Ps lifetime.

For PHBV polymer system, all of the PAL spectra were analyzed into three mean lifetimes, intensities, and also into lifetime distributions using PATFIT [32] and LT [33]. The shortest lifetime ($\tau_1 \approx 0.125$ ns) is the lifetime of *p*-Ps (the singlet state of Ps), and the intermediate lifetime ($\tau_2 \approx 0.4$ ns) is the lifetime of the free positron. The longest lifetime ($\tau_3 \approx 2$–3 ns) is due to the pick-off annihilation of *o*-Ps (triplet Ps). In this study, the lifetime and intensity were presented as the results determined from PATFIT program. The given value of τ_3 denotes the discrete values. In addition, an average τ_3 value of the log-normal distribution and its standard deviation (dispersion of the mean lifetime) can be determined by using LT program, which is in the distribution mode assumed that the annihilation rate λ follows a log-normal distribution function for a determined number of the annihilation channels. The value of τ_3 determined from LT was similar but smaller than the discrete values determined from PATFIT. A difference obtained between the τ_3 values determined from different analysis methods can be understood and has been discussed in the literatures [17,18]. In addition, there is no indication for the appearance of a shorter *o*-Ps lifetime ($\sim$1 ns) component from LT analysis. It could be concluded that Ps is not formed in crystal due to dense packing of PHBV molecular chains. *o*-Ps only annihilated at free volume holes in the amorphous phase including RAF and MAF regions, expected to have different size and distributions of free volume holes. However, free volume sizes in both RAF and MAF phases are too close to separate into two distributions due to the limited resolution of positron experiments. In consequence, the distributed lifetime showed a broad dispersion (>0.65 ns) and the mean lifetime indicated the average free volumes in both disordered regions.

Using *o*-Ps lifetime, the average free-volume hole-size assumed a spherical shape could be obtained by the following semi-empirical equation [9,34]:

$$\tau_3 = \frac{1}{2}\left[1 - \frac{R}{R_0} + \frac{1}{2\pi}\sin\left(\frac{2\pi R}{R_0}\right)\right]^{-1} \quad (1)$$

where τ_3 (*o*-Ps lifetime) and R (hole radius) are expressed in ns and Å, respectively. R_0 equals to $R + \Delta R$, where ΔR is the fitted empirical electron layer thickness (= 1.66 Å) [9]. Then, the volume of free-volume holes, V_f (Å^3), can be calculated:

$$V_f = \frac{1}{3}\left(4\pi R^3\right) \quad (2)$$

The *o*-Ps pick-off annihilation intensity (I_3) depends on the probability of *o*-Ps formation and the number density of free-volume holes. It is related to the radiation chemistry in which the *o*-Ps pick-off takes place. Due to the complexity of the *o*-Ps formation, the value of I_3 may be affected by other parameters. Therefore, some literatures reported that I_3 did not have a clear relation to the free volume properties [35,36]. However, in our previous report [37], we found that the *o*-Ps lifetime (τ_3) of a serious of PHBV membranes with different crystallinity, which was controlled by the crystallization process, was much close to each other at lower measuring temperature but I_3 decreased with increasing crystallinity. In the linear correlation between I_3 and crystallinity, we were able to observe extrapolated intercept, I_3 closed to 0% at 100% crystallinity. Many researchers also observed this behavior and suggested that the pick-off annihilation of *o*-Ps occurred only within the amorphous regions [17,29,38]. It can be concluded that I_3 is proportional to the number density of free-volume holes. In our system, the results of PAL analysis were discussed for the PHBV membranes prepared by different crystallization processes which changed the physical structure of PHBV polymer only. Herein, we assumed that the effect of radiation chemistry difference on the value of I_3 was very small due to the same chemical structure among the PHBV membranes and care was taken to avoid anomalous changes in I_3 which arose due to radiation damage; therefore, we assigned I_3 to represent the number density of free-volume holes of the PHBV membranes.

In order to compare the fractional free volume (FFV) of PHBV between the membranes with different crystallinity, both the variation of free volume size and the number density of free-volume holes should be considered. The relative fractional free volume (FFV) is expressed as follows:

$$\mathrm{FFV} = CV_fI_3 \quad (3)$$

where FFV is the fraction (%) of the free volume in the polymer, I_3 (%) is the *o*-Ps intensity. C is an empirical constant determined from the specific volume expansion coefficients of epoxy [39,40]. Herein, FFV from the PAL result should be considered as a relative value for the polymer of the same series since Eq. (3) was derived based on the Williams–Landel–Ferry (WLF) theory [39]. In common polymers, the value of C ranges from 0.001 to 0.002 [40]. However, a precise determination of C becomes difficult for semi-crystalline polymers because the thermal history varies the degree of crystallinity [39]. Hence, the relative fractional free volume was expressed by the product of V_f and I_3 only due to uncertain C parameter for semi-crystalline PHBV polymer. A product of mean volume of holes (V_f) and I_3, which is well accepted in literatures [6,41–43], is used to present the relative FFV. Although there are other arguments against relating I_3 with FFV since I_3 is affected by radiation chemistry of polymer systems [35,44], the I_3 value of PHBV polymer should still be included into the calculation of FFV to explain the effect of crystallinity on the FFV of PHBV membranes in our system due to the variation of I_3 with the crystallinity of the membranes. Otherwise, the data of PHBV membranes could not be explained well if one ignores the I_3 part in calculating FFV. A good linearity between crystallinity and relative FFV (V_fI_3) suggested that the *o*-Ps intensity plays an important role in the characterization of free volume properties [37]. Therefore, a product of V_f and I_3 is used to show the relative FFV of PHBV membranes in this manuscript.

Fig. 7 shows the longest lived lifetime component (τ_3, *o*-Ps lifetime) as a function of temperature during heating process. From the results of both computing programs, PATFIT and LT, the change of τ_3 values with temperature showed the same trend. Based on Eq. (1), the radius of free-volume hole could be calculated as appeared in the right *y*-axis of Fig. 7. It was observed that the free volume size increased with temperature linearly up to 110 °C. The thermal expansion coefficient of the free volume above 25 °C in the rubbery state (glass transition temperature (T_g) ~ 0 °C), α_{fv}, is calculated using Eqs. (2) and (4):

$$\alpha_{fv} = \left(\frac{1}{V_f}\right)\left(\frac{dV_f}{dT}\right) \tag{4}$$

The value of the α_{fv} of the free volume based on the mean volume of free volume holes (V_f) at 25 °C is found to be $1.19 \pm 0.09 \times 10^{-2}\ K^{-1}$. With the PAL data, the thermal expansion coefficient of the bulk polymer can be calculated by:

$$\alpha_{bulk} = FFV \cdot \alpha_{fv} + (1 - FFV) \cdot \alpha_{occ} \tag{5}$$

where FFV is the fractional free volume determined by Eq. (3) while the *C* constant ranges from 0.001 to 0.002 for common polymers. The thermal expansion coefficient of the occupied volume, α_{occ}, is $1.4 \times 10^{-4}\ K^{-1}$ [45]. It is calculated from the thermal expansion of unit cell parameter *a* of PHB crystal lattices from WAXD method because identical values of the unit cell parameters exist in PHBV polymer with 5% HV content. Although FFV is a function of temperature, the value of the FFV at 25 °C was chosen as a basis to calculate the thermal expansion coefficient of the bulk in Eq. (5) and the basis was consistent with the calculation of the thermal expansion coefficient of the free volume. The calculated α_{bulk} of PHBV is from $2.9 \times 10^{-4}\ K^{-1}$ to $4.5 \times 10^{-4}\ K^{-1}$ (depending on *C*). Comparing with other methods, the thermal expansion coefficient of PHBV with 13% HV is about $2 \times 10^{-4}\ K^{-1}$ which was determined by the use of a thermomechanical analyzer (TMA) with an expansion probe [46]. This demonstrates that PAL analysis provides a reasonable value for PHBV polymer.

In Fig. 7, τ_3 shows a linear increase up to 110 °C, followed by a plateau beyond 130 °C until completed melting. As observed here, at a certain temperature above T_g, Stevens et al. [47] denoted it as the "knee" temperature T_k, a distinct change in the thermal behavior of the free volume occurs. The increase of the volume of free-volume holes (V_f) with *T* slows down and levels off finally, indicated by the decrease of $dV_f(T)/dT$ toward zero. The leveling-off of *o*-Ps lifetime (τ_3) has already been observed previously [14,18,47,48]; however, is not well understood.

Frequently, the leveling-off effect is attributed to the formation of Ps bubble in the liquid-like state of a polymer. Because of the high mobility of polymer segments it is expected that a Ps can create a new open space [11]. The bubble size is determined by a balance of forces between the Ps-molecule repulsion and the microscopic surface tension. In addition, Dlubek et al. [18,30] interpreted the "knee" as being due to the thermal stimulation of various motional and vibrational processes with relaxation time near or below the *o*-Ps lifetime. When the relaxation times are significant longer than the *o*-Ps lifetime (τ_3 ~ 2 ns), the polymer dynamics do not change the size and shape of free volume during the *o*-Ps life. Molecular motions with relaxation times smaller than τ_3, however, cause a smearing in the molecule and electron density distribution during the *o*-Ps life and effectively raise the electron density in the free volume, or decrease the empty space inside a hole. Under favorable conditions the increase of τ_3 with the free volume on heating can be overweighed by the decrease of space inside free volume holes caused by the thermal motion. For even stronger thermal motion, a decrease in the observed *o*-Ps lifetime could be imagined. The Ps bubble effect might stabilize the local empty space sensed by the Ps probe.

The free volume size distribution was described by the dispersion of mean lifetime, which is the standard deviation of the mean lifetime caused by the log-normal distribution, as shown in Fig. 8. Not surprisingly, the same tendency of the dispersion of *o*-Ps lifetime as that of the *o*-Ps mean lifetime was observed. Ps bubble formation or the thermal stimulation may be the reasons causing the size distribution of free-volume hole maintains in a certain range above T_k as discussed above.

However, neither Ps bubble effect nor fast motional process can completely interpret the thermal behavior of *o*-Ps lifetime of PHBV as shown in Fig. 7. It is noticed that the *o*-Ps lifetime appears a distinct increase at 190 °C which is higher than T_m and the transition to a homogeneous liquid occurs here. The Ps bubble might not form at early stage of thermal expansion process near 130 °C. Possibly, the local free volume detected by PALS may mirror the structural transition of polymer chains.

In addition, *o*-Ps intensity shows an increased trend on the heating process until to the melting (see in Fig. 9). The *o*-Ps intensity was at a relatively constant value in the range from room temperature to around 70 °C and then increased rapidly after 70 °C.

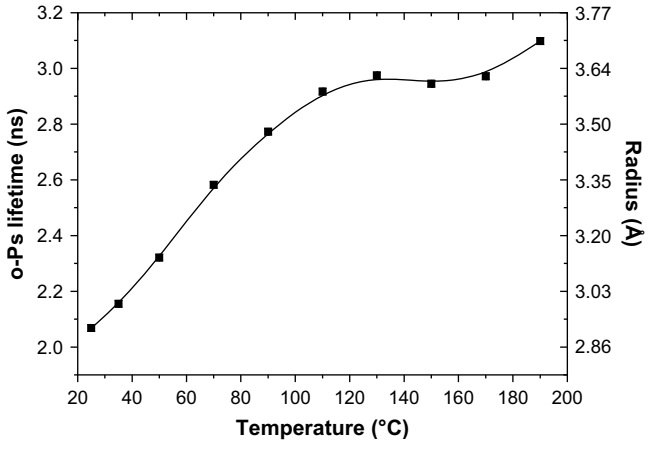

Fig. 7. Temperature dependence of the *o*-Ps lifetime of the 90 °C isothermally crystallized PHBV membrane.

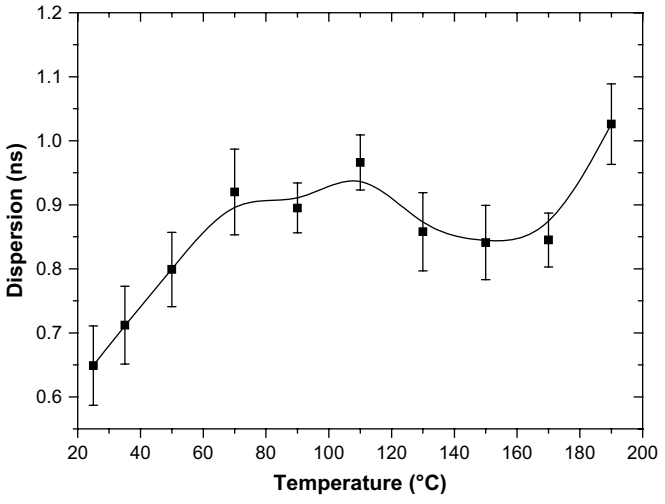

Fig. 8. Temperature dependence of the *o*-Ps lifetime distribution of the 90 °C isothermally crystallized PHBV membrane.

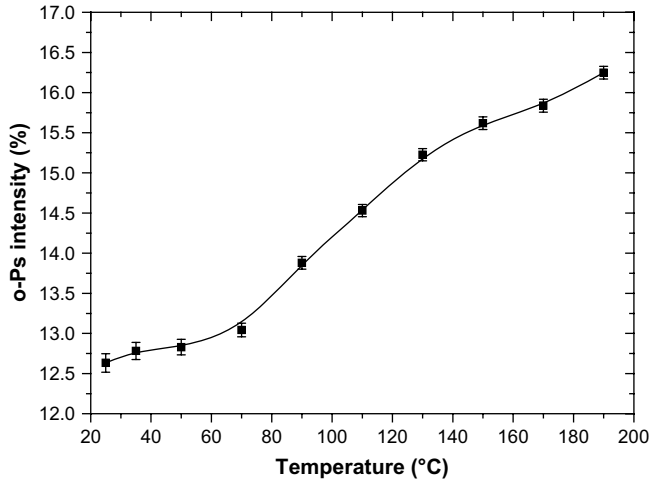

Fig. 9. Temperature dependence of the *o*-Ps intensity of the 90 °C isothermally crystallized PHBV membrane.

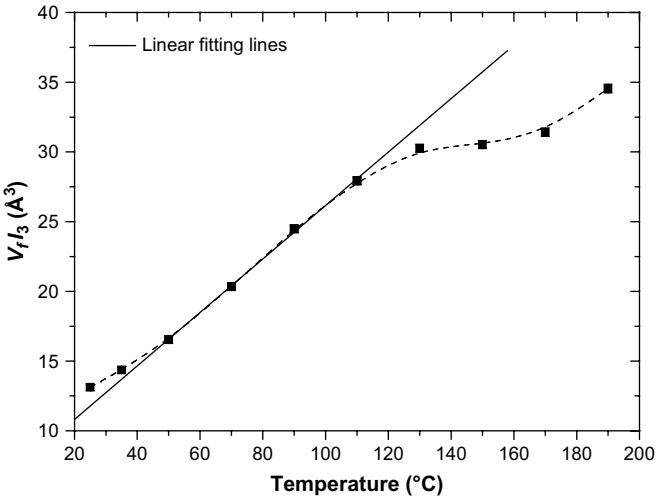

Fig. 11. Temperature dependence of the relative FFV ($V_f I_3$) of the 90 °C isothermally crystallized PHBV membrane.

These observations are related to the structure of semi-crystalline polymers. A simple two-phase model, crystallites embedded in amorphous surroundings, is not sufficient to correlate the properties. The non-crystalline phase must be subdivided into the mobile amorphous fraction (MAF) and the rigid amorphous fraction (RAF). The existence of RAF was often associated with the regions in the lamellar stacks; where the crystalline lamellae are separated by very thin (2–4 nm) amorphous layers. Much thicker (10–200 nm) amorphous layers separate the lamellar stacks [49,50]. It is suggested that RAF is associated with the interlamellar regions, while MAF is associated with the interstack amorphous regions [51]. For the PHBV membrane which was isothermally crystallized at 90 °C, the immobilization of the amorphous material around less perfect crystals results in the vitrification of the RAF during crystallization. According to the results of DSC trace of the PHBV membrane, a transition state of the RAF was observed due to the devitrification of the RAF between 40 and 80 °C as shown in Fig. 10. With a further increase of temperature, the mobility of segment at fold surface of the crystallites would increase observably. It leaded to the rearrangement of molecular chain packing above this temperature so that new free volume holes were created, the *o*-Ps intensity increased from 13.88 to 16.25% when the measuring temperature increased from 90 °C to 190 °C.

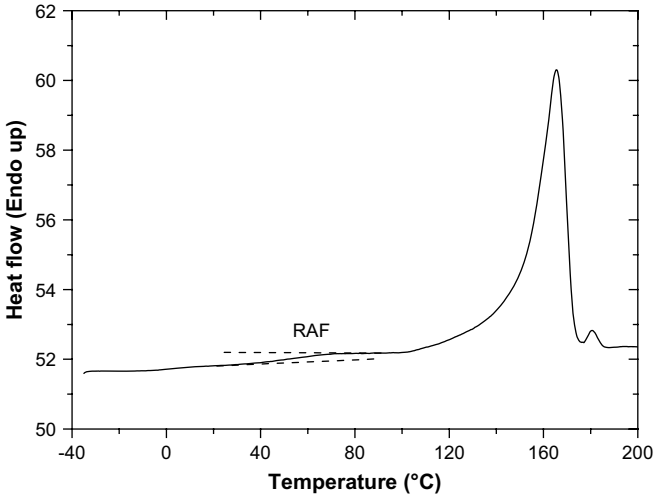

Fig. 10. DSC curves of the 90 °C isothermally crystallized PHBV membrane.

In Fig. 11, the relative fractional free volume (FFV, $V_f I_3$) presents a dependence on temperature. Similar to the *o*-Ps lifetime, the thermal expansion of free volume shows a linear behavior from 45 to around 120 °C. According to the structural analysis of PHBV polymer by FTIR, a pre-melting behavior appeared above 130 °C during the heating process (see in Fig. 3). On heating, the constrained RAF near the crystals should disappear as soon as the less perfect or small crystals melt. Even the *o*-Ps lifetime estimated by PAL could not represent the real free volume hole size on the melting process, the devitrification of the RAF would create more number of local free volume holes, so that the FFV increased continually but the slope slowed down above 130 °C.

4. Conclusion

A novel technique – positron annihilation lifetime (PAL) spectroscopy is used to measure the free volume properties of semi-crystalline PHBV membrane and provide significant structure information at molecular level. The temperature dependence and the melting behaviors of the free volume of crystallized PHBV membrane were first studied by PAL spectroscopy. Although the *o*-Ps lifetime increased with temperature by a rapid increase in its slope from room temperature, the *o*-Ps intensity increased slightly until temperature was higher than 70 °C. The width of *o*-Ps lifetime distribution increased with temperature parallel to the increase of *o*-Ps lifetime. At a "knee" temperature T_k, the increases in the *o*-Ps lifetime and the lifetime distribution leveled off. Fast motional processes and/or the Ps bubble formation in the liquid-like state of a polymer were discussed as possible reasons for these effects. Furthermore, this knee represented the onset of the partial melting similar to the results observed in FTIR, while the helical structure broke up partially above 130 °C. It is concluded that the local free volume detected by PALS might mirror the structural transition of polymer chains.

The formulation of three-phase model, which included crystalline, RAF, and MAF phases, was addressed to interpret the free volume characteristics of melt-crystallized PHBV membranes. The behaviors of the annihilation parameters, including τ_3, I_3, size distribution, and FFV, and thermal expansion of crystallized PHBV could be understood assuming that a fraction of the amorphous

phase, so-called RAF, became restricted in its segmental mobility due to the incorporation of polymer chains into the crystals during crystallization.

Acknowledgments

This work was supported by the National Science Council of the Republic of China through the grants of NSC95-2218-E-155-001 and NSC96-2221-E-155-074.

References

[1] Verhoogt H, Ramsay BA, Favis BD. Polymer 1994;35:5155.
[2] Cox MK. Biodegradable plastic and polymers. Elsevier; 1994.
[3] Miguel O, Barbari TA, Iruin JJ. J Appl Polym Sci 1999;71:2391.
[4] Miguel O, Iruin JJ. J Appl Polym Sci 1999;73:455.
[5] Philip S, Keshavarz T, Roy I. J Chem Technol Biotechnol 2007;82:233.
[6] Chen H, Cheng ML, Jean YC, Lee LJ, Yang J. J Polym Sci Part B Polym Phys 2008;46:388.
[7] Dlubek G, Gupta AS, Pionteck J, Häßler R, Krause-Rehberg R, Kaspar H, et al. Polymer 2005;46:6075.
[8] Jean YC, Mallon PE, Schrader DM. Principles and application of positron and positron chemistry. Singapore: World Scientific; 2003.
[9] Nakanishi H, Wang SJ, Jean YC. Positron annihilation studies of fluids. Singapore: World Scientific; 1988.
[10] Yampolskii Y, Shantarovich V. Materials science of membranes for gas and vapor separation. New York: Wiley Interscience; 2006.
[11] Mogensen OE. Positron annihilation in chemistry. Berlin: Springer-Verlag; 1995.
[12] Suzuki H, Grebovicz J, Wunderlich B. Br Polym J 1985;17:1.
[13] Hu YS, Liu RYF, Zhang LQ, Rogunova M, Schiraldi DA, Nazarenko S, et al. Macromolecules 2002;35:7326.
[14] Kilburn D, Bamford D, Lüpke T, Dlubek G, Menke TJ, Alam MA. Polymer 2002;43:6973.
[15] Lin J, Shenogin S, Nazarenko S. Polymer 2002;43:4733.
[16] Machado J, Silva GG, De Oliveira FC, Lavail RL, Rieumont J, Licinio P, et al. J Polym Sci Part B Polym Sci 2007;45:2400.
[17] Dlubek G, Stejny J, Lüpke T, Bamford D, K.P, Hübner C, et al. J Polym Sci Part B Polym Sci 2002;40:65.
[18] Dlubek G, Supei M, Bondarenko V, Pionteck J, Pompe G, Krause-Rehberg R, et al. J Polym Sci Part B Polym Sci 2003;41:3007.
[19] Kilburn D, Bamford D, Dlubek G, Pionteck J, Alam MA. J Polym Sci Part B Polym Sci 2003;41:3089.
[20] Tashiro K, Sasaki S, Gose N, Kobayashi M. Polym J 1998;30(6):485.
[21] Xu J, Guo B-H, Yang R, Wu Q, Chen G-Q, Zhang Z-M. Polymer 2002;43:6893.
[22] Yoshie N, Asaka A, Yazawa K, Kuroda Y, Inoue Y. Polymer 2003;44:7405.
[23] Wu Q, Tian G, Sun SQ, I.N, Chen GQ. J Appl Polym Sci 2001;82:934.
[24] Bayari S. New biomedical materials: basic and applied studies. IOS Press; 1998.
[25] Bayari S, Severcan F. J Membr Struct 2005;744–747:529.
[26] Zhu XY, Yan DY. Macromol Chem Phys 2001;202(7):1109.
[27] Madani MM, Macqeen RC, Granata RD. J Polym Sci Part B Polym Sci 1996; 34:2770.
[28] Tanaka M, Takebe K, Uedono A, Ujihira Y, Horie K, Asanuma T. Mater Sci Forum 1992;105–110:1737.
[29] Nakanishi H, Jean YC, Smith EG, Sandreczki TC. J Polym Sci Part B Polym Phys 1989;27:1419.
[30] Dlubek G, Redmann F, Krause-Rehbrg R. J Appl Polym Sci 2002;84:244.
[31] Li HL, Ujihira Y, Shukushima S, Uedono K. Polymer 2000;41:92.
[32] PATFIT package. Denmark: RN Laboratory; 1989.
[33] Kansy J. Nucl Instrum Methods Phys Res A 1996;374:235.
[34] Tao SJ. J Chem Phys 1972;56:5499.
[35] Dlubek G, Bondarenko V, Al-Qaradawi IY, Kilburn D, Krause-Rehberg R. Macromol Chem Phys 2004;205:512.
[36] Hirade T, Maurer FHJ, Eldrup M. Radiat Phys Chem 2000;58:465.
[37] Cheng ML, Sun YM. J Polym Sci B Polym Phys, in press.
[38] Muramatsu H, Matsumoto K, Minekawa S, Yagi Y, Sasai S. Radiochim Acta 2001;89:119.
[39] Jean YC. Microchem J 1990;42:72.
[40] Liu J, Deng Q, Jean YC. Macromolecules 1993;26:7149.
[41] Jobando VO, Quarles CA. Phys Stat Sol (c) 2007;4:3763.
[42] Olson BG, Lin J, Nazarenko S, Jamieson AM. Macromolecules 2003;36:7618.
[43] Lue SJ, Lee DT, Chen JY, Chiu CH, Hu CC, Jean YC, et al. J Membr Sci 2008; 325:831.
[44] Maurer FHJ, Schmidt M. Radiat Phys Chem 2000;58(5):509.
[45] Škrbić Ž, Divjaković V. Polymer 1996;37:505.
[46] Bhardwaj R, Mohanty AK, Drzal LT, Pourboghrat F, Misra M. Biomacromolecules 2006;7:2044.
[47] Stevens R, Chung SH, Horoyski P, Jeffrey KR. J Non-Cryst Solids 1994;172–174:1207.
[48] Schick C, Wurm A, Mohamed A. Colloid Polym Sci 2001;279:800.
[49] Lovinger AJ, Hudson SD, David DD. Macromolecules 1992;25:1992.
[50] Santa Cruz C, Stribeck N, ZH G, BCF J. Macromolecules 1991;24:5980.
[51] Sauer BB, Hsiao BS. Polymer 1995;36:2553.